DMD Fast Forward. Published on September 20, 2006 as doi:10.1124/dmd.106.012054

DMD # 12054

Engineering of Cytochrome P450 3A4 for Enhanced Peroxide-mediated Substrate Oxidation Using Directed Evolution and Site-directed Mutagenesis

Santosh Kumar, Hong Liu, and James R. Halpert

Department of Pharmacology and Toxicology,

University of Texas Medical Branch,

301 University Blvd.,

Galveston, Texas (S.K. and J.R.H.)

The Center for Drug Discovery and Design

Shanghai Institute of Material Medica

Chinese Academy of Sciences

555 Zu Chong Zhi Road,

Zhangjiang Hi-Tech Park,

Shanghai 201203, China (H. L.)

Running Title: Designing P450 3A4 for Enhanced Peroxide-supported Activity

Corresponding Author:

Santosh Kumar, Department of Pharmacology and Toxicology, University of Texas Medical Branch, 301 University Boulevard, Galveston, TX 77555-1031

Tel: (409) 772-9677, Fax: (409) 772-9642, Email: sakumar@utmb.edu

Number of text pages: 43

Number of Tables: 6

Number of Figures: 5

Number of References: 41

Number of words in Abstract: 236

Number of words in Introduction: 493

Number of words in Discussion: 1538

Abbreviations:

CYP3A4, Cytochrome P450 3A4; PCR, Polymerase chain reaction; 7-BQ, 7-Benzyloxyquinoline; 7-BFC, 7-Benzyloxy-4-(trifluoromethyl)coumarin; 7-HQ, 7-Hydroxyquinoline; 7-HFC, 7-Hydroxy-4-(trifluoromethyl)coumarin; SRS, Substrate recognition site; CPR, NADPH-cytochrome P450 reductase; b_5, Cytochrome b_5; HOOH, Hydrogen peroxide; CuOOH, Cumene hydroperoxide

Abstract

Cytochrome P450 3A4 (CYP3A4) has been subjected to random and site-directed mutagenesis to enhance peroxide-supported metabolism of several substrates. Initially, a high-throughput screening method using whole cell suspensions was developed for H_2O_2-supported oxidation of 7-benzyloxyquinoline (7-BQ). Random mutagenesis by error-prone PCR and activity screening yielded several CYP3A4 mutants with enhanced activity. L216W and F228I showed a 3-fold decrease in $K_{m,\ HOOH}$ and a 2.5-fold increase in $k_{cat}/K_{m,\ HOOH}$ compared with CYP3A4. Subsequently, T309V and T309A were created based on the observation that T309V in P450 2D6 has enhanced cumene hydroperoxide (CuOOH)-supported activity. T309V and T309A showed a > 6- and 5-fold higher $k_{cat}/K_{m,\ CuOOH}$ than CYP3A4, respectively. Interestingly, L216W and F228I also exhibited a > 4- and > 3-fold higher $k_{cat}/K_{m,\ CuOOH}$ than CYP3A4, respectively. Therefore several multiple mutants were constructed from rationally designed and randomly isolated mutants; among them F228I/T309A showed an 11-fold higher $k_{cat}/K_{m,\ CuOOH}$ than CYP3A4. Addition of cytochrome b_5, which is known to stimulate peroxide-supported activity, enhanced the $k_{cat}/K_{m,\ CuOOH}$ of CYP3A4 by 4- to 7-fold. When the mutants were tested with other substrates, T309V and T433S showed enhanced $k_{cat}/K_{m,\ CuOOH}$ with 7-benzyloxy-4-(trifluoromethyl)coumarin (7-BFC) and testosterone, respectively, compared with CYP3A4. In addition, in the presence of cytochrome b_5 T433S has the potential to produce milligram quantities of 6β-OH testosterone through peroxide-supported oxidation. In conclusion, a combination of random and site-directed mutagenesis approaches yielded CYP3A4 enzymes with enhanced peroxide-supported metabolism of several substrates.

DMD Fast Forward. Published on September 20, 2006 as DOI: 10.1124/dmd.106.012054
This article has not been copyedited and formatted. The final version may differ from this version.

Mammalian cytochromes P450 comprise a ubiquitous superfamily of heme-containing enzymes, which perform a variety of oxidative reactions on a wide range of substrates including > 90% drugs and environmental pollutants (Coon, 2005). P450-derived metabolites are often biologically active themselves, and understanding their effects is crucial in evaluating a drug's efficacy, toxicity, and pharmacokinetics (Johnson et al., 2004). Such studies, however, can require large quantities of the pure metabolites, which may be difficult to synthesize. An alternate approach is to use human P450s to generate the metabolites of drugs and drug candidates. Limitations include poor activity, stability, and expression of P450s in *E. coli*. In addition, a troublesome reconstitution of P450s, which involves NADPH-cytochrome P450 reductase (CPR), often cytochrome b_5 (b_5), and phospholipids concurrent with an expensive cofactor, NADPH, further limits their application in synthesis. Therefore, designing xenobiotic-metabolizing P450s with enhanced activity, stability, and expression, and which utilize an alternate oxygen donor such as hydrogen peroxide (H_2O_2) or cumene hydroperoxide (CuOOH), is highly desirable (Kumar and Halpert, 2005).

Cytochrome P450 3A4 (CYP3A4) is the most abundant P450 enzyme in human liver and metabolizes a wide variety of drugs (> 50%) and carcinogens (Guengerich, 1999; Nebert and Russell, 2002). Because of its pharmacological and environmental significance, CYP3A4 has been the subject of a large number of structure-function studies involving X-ray crystallography, protein modeling, and site-directed mutagenesis (Domanski and Halpert, 2001; Hutzler and Tracy, 2002; Ekins et al., 2003; Tanaka et al., 2004; Williams et al., 2004; Yano et al., 2004; Park et al., 2005; Scott and Halpert, 2005). However, no attempt has been made to engineer CYP3A4 for enhanced catalytic activity,

especially in a peroxide system. More recently, microsomal and *E. coli* expressed CYP3A4-CPR with an NADPH generating system has been used to produce drug metabolites in milligrams quantities (Vail et al., 2005).

Over the past decade, directed evolution has been used successfully to design industrial biocatalysts for enhanced catalytic efficiency, stability, and versatility (Schoemaker et al., 2003; Gillam, 2005). Exciting recent results with the bacterial enzyme P450BM3 have illustrated the potential of directed evolution for engineering P450s that utilize artificial oxygen donors (Glieder et al., 2002; Meinhold et al., 2005). Recently, P450 BM3 has been engineered by directed evolution to produce the authentic human metabolites of propranolol (Otey et al., 2006). Directed evolution of several mammalian P450s for enhanced activity has been established (Kim and Guengerich, 2004) and their potential applications have been reviewed recently (Kumar and Halpert, 2005). In addition, we have developed a directed evolution approach to engineer P450 2B1 for enhanced H_2O_2-supported 7-ethoxy-4-trifluoromethylcoumarin *O*-deethylation (Kumar et al., 2005a). In the present study we have engineered CYP3A4 using the combination of directed evolution and site-directed mutagenesis for enhanced utilization of peroxide. The most efficient enzyme, F228I/T309A, shows a > 11-fold higher $k_{cat}/K_{m,\ CuOOH}$ than CYP3A4 for 7-BQ debenzylation. In addition, an engineered enzyme T433S can metabolize testosterone more efficiently than CYP3A4 and has the potential to produce milligrams quantity of 6β-OH testosterone.

Materials and Methods

Materials. 7-BQ, 7-BFC (7-benzyloxy-4-(trifluoromethyl)coumarin), 7-HQ (7-hydroxyquinoline), and 7-HFC (7-hydroxy-4-(trifluoromethyl)coumarin) were purchased from Molecular Probes, Inc. (Eugene, OR). Polymyxin B sulfate, H_2O_2, CuOOH, and NADPH were bought from Sigma Chemical Co. (St. Louis, MO. [4-^{14}C]-testosterone was obtained from Amersham Biosciences (Piscataway, NJ). Recombinant CPR and b_5 from rat liver were prepared as described previously (Harlow and Halpert, 1997). Oligonucleotide primers for polymerase chain reaction (PCR) were either obtained from the UTMB Molecular Biology Core Laboratory (Galveston, TX) or from Sigma Genosys (Woodlands, TX). Error-prone PCR and ligation kits were obtained from Roche (Indianapolis, IN). The QuikChange XL site-directed mutagenesis kit was obtained from Stratagene (La Jolla, CA). Ni-NTA affinity resin was purchased from Qiagen (Valencia, CA). All other chemicals were of the highest grade available and were obtained from standard commercial sources.

Random mutagenesis by error-prone PCR and construction of mutant libraries. Random mutagenesis was essentially performed using error-prone PCR of the cDNA as described previously for P450 2B1 (Kumar et al., 2005a). Initially, error-prone PCR was standardized to ensure a mutation rate of 1-2 bp per P450 by using 25 mM $MgCl_2$, 10 mM dCTP, 10 mM dTTP, and 2 mM each of dATP and dGTP (Cirino et al., 2003). Subsequently, ligation and transformation were standardized in order to obtain > 1000 clones per PCR reaction by selecting suitable forward and reverse primers (Fig. 1),

restriction sites (*NcoI/Kpn*I), ligation conditions (overnight ligation kit), and transformation procedures (commercial XL-Blue *E. coli*).

Site-directed Mutagenesis. T309A, T309I, and T309F were created as described (Domanski et al., 2001). While T309V was created using CYP3A4 as a template, other multiple mutants were created using a single/double mutant as a template and appropriate forward and reverse primers as presented in Figure 1. To confirm the desired mutation and verify the absence of unintended mutations all constructs were sequenced at the University of Texas Medical Branch Protein Chemistry Laboratory (Galveston, TX).

Screening and selection. Screening and selection of random mutants were essentially done as described previously for P450 2B1 (Kumar et al., 2005a). Liquid handling was performed using a multi-channel robot Biomek 2000 (Beckman, Fullerton, CA). In brief, transformed *E. coli* was grown in a 300 µl, V-shaped 96-well microplate containing 150 µl LB media for 18-20 h at 30 ^{o}C on a microplate shaker. Next, 20 µl of the LB grown cells were inoculated into a 300 µl, V-shaped 96-well microplate containing 180 µl TB medium and grown for ~3 h until the cell density reached $O.D._{600}$ = 1-1.5. δ-aminolevulinic acid and IPTG were then added to the cells to final concentrations of 80 and 240 µg/ml, respectively. The cells were then grown for 48 h at 30 ^{o}C on a microplate shaker. Cells were then harvested by centrifugation at 5000 g for 10 min using an Allegra 25R microplate centrifuge (Beckman). The supernatant was removed by decanting, and the pellet was dried. The cells were resuspended in 150 µl of 0.1 M Hepes buffer, pH 7.4, which is termed whole cells.

Next, 50 µl of the substrate mixture (400 µM 7-BQ containing 4% methanol and 5 U/well polymyxin B sulfate, respectively) was incubated with 40 µl of whole cells for 5 min at room temperature. The background intensity was recorded at λ_{ex} = 405 nm and λ_{em} = 510 nm using a fluorescence microplate reader (Ascent Fluoroscan, Ramsey, MN). The reaction was initiated by the addition of 10 µl H_2O_2 (10 mM final concentrations), and the formation of product was recorded at 2.5 min. Mutants with ≥ 2-fold higher activity than the average template activity were sequenced at the UTMB Protein Chemistry Laboratory and were further characterized as described below.

Expression and purification of wild-type and engineered enzymes. CYP3A4 and mutants were expressed as His-tagged proteins in *E. coli* TOPP3 and purified using a Ni-affinity column as described previously (Domanski et al., 2001). Protein concentrations were determined using the Bradford protein assay kit (BioRad, Hercules, CA). The specific contents of wild-type and most random mutants were between 10 and 15 nmol of P450 per mg protein. Upon purification, the yield, purity, and stability of the random mutant proteins were either similar to or higher than the wild-type enzyme. T309V, T309A/L216W, and F228I/F241V showed low P450 expression (< 40 nmol/l), high P420 (> 75%), and low specific content (< 4.0 nmol of P450 per mg protein). L216W/T309V and F228I/T309V showed very low P450 expression (> 10 nmol/l), and were not purified for further study.

Enzyme assays. H_2O_2- and CuOOH-supported enzyme activities were assayed as described previously with slight modifications (Kumar et al., 2005a; Kumar et al.,

2005b). Substrate mixtures were prepared in 100 mM Hepes buffer, pH 7.4, with 2% as the final concentration of methanol (100 µl/well of a 96-well microplate). The substrate mixture was pre-incubated with 25 or 50 pmol of purified P450 enzyme at room temperature for 5 min. Reactions were initiated by the addition of H_2O_2 (10 mM) or CuOOH (2.5 mM). For steady-state kinetics with the peroxide, different concentrations of H_2O_2 (1 - 25 mM) or CuOOH (0.05 - 2.5 mM) were used at 200 µM of 7-BQ. After 3 min of incubation, the reactions were stopped by adding 340 units (50 µl) of catalase. Subsequently, 50 µl of 100 mM Hepes buffer, pH 7.4 was added prior to recording the fluorescence intensity at λ_{ex} = 405 nm and λ_{em} = 510 nm using an Ascent fluorescence plate reader. For 7-BFC *O*-deethylation and testosterone 6β-hydroxylation 75 µM and 200 µM of the substrates, respectively, were incubated with the enzyme systems before initiating the reactions using appropriate concentrations of CuOOH as described above. Testosterone hydroxylation was assayed by TLC using radiolabeled substrate (Kumar et al., 2005a), while 7-BFC oxidation was assayed using a fluorescence method (Domanski et al., 2001). To determine the effect of b_5, a 1:1 molar ratio of P450 and b_5 at 0.25 µM P450 were incubated for 10 min prior to incubating with substrates.

The standard NADPH-dependent assays with 7-BQ, 7-BFC, and testosterone were essentially carried out as described (Domanski et al., 2001; Kumar et al., 2003). The reconstitution system contained CYP3A4, CPR and b_5 at ratios of 1:4:2 and included 10 µg DOPC/100 µl reaction volume.

Steady state kinetic parameters were determined by regression analysis using Sigma Plot (Jandel, San Rafel, CA). The K_m value was determined using the Michaelis-Menten equation, whereas the S_{50} and n values were determined using the Hill equation.

Each kinetic experiment included CYP3A4 and mutants (presented in Tables 1-6) simultaneously using a high throughput microplate assay for more accurate comparison of the data. The standard errors for fit to Michaelis-Menten or Hill equations were large when the $K_{m,\ HOOH}$ or $S_{50,\ 7\text{-}BQ}$ is higher than the maximum concentration of the reactants used.

P450 heme-depletion assay. Determination of the kinetics of CYP3A4 heme depletion in the presence of CuOOH was done as previously described for H_2O_2 (Kumar et al., 2005b). In brief, the reaction was carried out at 25 °C in 100 mM Hepes buffer, pH 7.4, in a 1-ml semi-micro spectrophotometric cell with constant stirring. The reaction mixture contained 1 μM P450 and different concentrations of CuOOH (0.01 - 15 mM). Bleaching of the hemoprotein was followed by measuring a series of absorbance spectra using Shimadzu-2600 spectrophotometer in the 340-700 nm range. Fitting of the titration curves were performed by regression analysis using Sigma Plot (Jandel, San Rafel, CA). A simple pseudo-first order equation was used to determine the k_{inact} values at different CuOOH concentrations, and a Michaelis-Menten equation was used to determine the $K_{I,\ CuOOH}$ value.

Results

Directed evolution of CYP3A4. The most critical step in directed evolution is to find a simple, economical, and high-throughput activity screen. Recently, we have developed a facile assay method to circumvent steps involving CPR and b_5 by using the alternate oxygen donor H_2O_2 for CYP3A4 (Kumar et al., 2005b). Because H_2O_2-supported activity with 7-BQ is very low in the wild-type, several existing CYP3A4 mutants were examined. Only L211F/D214E and L373F showed 1.5-fold higher activity than CYP3A4. However, L211F/D214E showed abolished enzyme cooperativity and L373F showed low expression and stability (data not shown). Therefore, CYP3A4 was used as the template for directed evolution. The activity screen was optimized using whole cell suspensions as described earlier for P450 2B1 (Kumar et al., 2005a). 10 mM H_2O_2 was used for screening mutants using whole cell suspensions because above this concentration the reaction is not linear up to 2.5 min (data not shown). A representative assay of multiple colonies of CYP3A4 indicated ~70% colony-to-colony variation in activity (Fig. 2, open triangles) compared with the average CYP3A4 colony. The control showed very low relative intensity (Fig. 2, open diamonds). These data suggested that random clones having ≥ 2-fold higher activity than CYP3A4 would correspond to mutants with enhanced catalytic activity.

Representative data from an initial screen of several thousand random clones derived from directed evolution of CYP3A4 are shown in Figure 2B, with the clones graphed in order of decreasing activity. Upon random mutagenesis we selected four clones that showed ≥ 2.5-fold higher activity than the average of CYP3A4. DNA sequencing revealed a single new mutation in each case, L216W, F228I, F241V, and

T433S. The mutants were then expressed in large scale culture and purified. These single mutants either showed higher or similar expression levels and very low P420 compared with CYP3A4, suggesting that the random mutants that are selected using activity screen maintain stability unlike many site-directed mutants (Kumar et al., 2003).

Steady-state kinetics at varying 7-BQ concentrations. To test whether the selected purified mutants also showed enhanced k_{cat}, steady-state kinetic analysis of 7-BQ oxidation at 10 mM H_2O_2 and at varying 7-BQ concentration was carried out. Above 10 mM, H_2O_2 accelerates heme depletion and the reaction is not linear up to 5 min (Kumar et al., 2005b). L216W, F228I, and T433S showed 60-80% higher k_{cat} values than CYP3A4 (Table 1). However, F241V showed only a 20% higher k_{cat} than CYP3A4. In addition, F228I showed a significant increase in the $S_{50,\ 7\text{-BQ}}$ and decrease in the n values. Subsequently, to test whether the increased k_{cat} in the H_2O_2-supported assay is also associated with an increased k_{cat} in the NADPH-supported reaction, the mutants were assayed in the standard reconstituted system using NADPH. All the mutants showed 10-40% lower k_{cat} than CYP3A4 with a significant change in the S_{50} and n values (Table 1). In this assay the accuracy of the S_{50} is limited by the highest 7-BQ concentration used. Overall, the results suggested that our screening method is limited to identification of CYP3A4 mutants with enhanced activity in the H_2O_2-supported system.

Steady-state kinetics at varying H_2O_2 concentrations. Subsequently, we sought to determine whether the screening method is targeted to increased k_{cat}, and/or decreased $K_{m,\ HOOH}$. Therefore, steady-state kinetic analysis at 200 μM 7-BQ and at varying H_2O_2

concentrations was carried out. At 20 mM H_2O_2 the rate of 7-BQ debenzylation is linear for up to 3 min (data not shown). CYP3A4 showed a very high $K_{m,\ HOOH}$ (61 mM), which is much higher than the H_2O_2 concentration used for the activity screening (10 mM) (Table 2). None of the mutants showed improvements in k_{cat}, whereas L216W and F228I showed ~3-fold decrease in the $K_{m,\ HOOH}$ values leading to > 2.5-fold enhancement in $k_{cat}/K_{m,\ HOOH}$ compared with CYP3A4. Compared with CYP3A4, F241V and T433S showed a modest increase in the $k_{cat}/K_{m,\ HOOH}$ values as the result of decreased $K_{m,\ HOOH}$ (Table 2). The results suggested that the screening method is selective for mutants with decreased $K_{m,\ HOOH}$. Furthermore, to test the hypothesis that the combination of single mutants would show a further enhancement in $k_{cat}/K_{m,\ HOOH}$, several multiple mutants were constructed. Unexpectedly, these multiple mutants did not show further improvement (Table 2). F228I/T43S and F241V/F228I showed similar $k_{cat}/K_{m,\ HOOH}$ values to F228I, whereas most multiple mutants showed decreased $k_{cat}/K_{m,\ HOOH}$, mainly as the result of decreased k_{cat}.

Steady-state kinetics at varying CuOOH concentrations: Recently, T309V has been shown to display higher activity than CYP2D6 wild-type in a CuOOH-supported reaction (Keizers et al., 2005). Therefore, the existing CYP3A4 mutants T309A, T309I, and T309F were assayed for CuOOH-supported 7-BQ debenzylation. At 200 μM 7-BQ and 2.5 mM CuOOH T309A showed a > 3-fold higher activity, whereas T309I and T309F demonstrated lower activity than CYP3A4. Subsequently, T309V was constructed by site-directed mutagenesis and showed a > 5-fold higher activity than CYP3A4. Therefore, steady-state kinetic analysis at 200 μM 7-BQ concentration and at varying

CuOOH concentrations was carried out with T309A and T309V. At 2.5 mM CuOOH the rate of 7-BQ debenzylation is linear for up to 5 min (data not shown). T309A and T309V exhibited a 4- and 6-fold higher $k_{cat}/K_{m,\ CuOOH}$, respectively, than CYP3A4 in CuOOH-supported reaction mainly as the result of increased k_{cat} values (Table 3). When steady-state kinetic analysis was performed in the H_2O_2-supported reaction, T309V exhibited a 2-fold higher $k_{cat}/K_{m,\ HOOH}$ than CYP3A4, whereas T309A showed lower $k_{cat}/K_{m,\ HOOH}$ than CYP3A4 (data not shown). In addition, T309A and T309V showed lower k_{cat} values in H_2O_2-supported than CuOOH-supported reactions. Furthermore, to test whether T309A and T309V in CYP3A4 follow a trend similar to T309V in CYP2D6 the standard NADPH-supported oxidation of 7-BQ was performed. T309A and T309V showed lower NADPH-supported activity than CYP3A4, as was found in the case of CYP2D6 (data not shown).

Subsequently, we tested individual single random mutants and multiple mutants for CuOOH-supported activity (Table 3). L216W and F228I exhibited > 3- and > 4.5-fold higher $k_{cat}/K_{m,\ CuOOH}$ than CYP3A4, respectively, whereas F241V and T433S exhibited ~ 2-fold higher $k_{cat}/K_{m,\ CuOOH}$ than CYP3A4. The results indicated that the random mutants that were isolated for decreased $K_{m,\ HOOH}$ also showed enhanced utilization of CuOOH ($k_{cat}/K_{m,\ CuOOH}$) mainly as the result of increased k_{cat} values compared with CYP3A4. As seen earlier with the H_2O_2-supported reaction, combination of these single random mutants did not improve the k_{cat}/K_m for CuOOH further. Therefore, T309A was added to the individual single random mutants to create several multiple mutants, and their activity was assayed in the CuOOH-supported reaction. Among the mutants with reasonable expression (see Material and Methods),

F228I/T309A showed the highest k_{cat}/K_m for CuOOH, which was 2-fold higher than T309A and 11-fold higher than CYP3A4 (Table 3). Interestingly, the K_m for CuOOH was lower by more than an order of magnitude than the K_m for H_2O_2 (~1.0 mM vs. 20-60 mM).

Effect of cytochrome b_5 on CuOOH-supported oxidation of 7-BQ. To investigate whether b_5 also stimulates CuOOH-supported 7-BQ oxidation by CYP3A4, as shown earlier for H_2O_2 (Kumar et al., 2005b), steady-state kinetic analysis was performed at varying CuOOH concentrations and at 200 μM 7-BQ. Cytochrome b_5 stimulated $k_{cat}/K_{m, CuOOH}$ by 7-fold in CYP3A4, and by > 5-fold in random mutants (Table 3 vs. Table 4). However, the site-directed mutants T309A and T309V showed relatively less stimulation by b_5. In F228I/T309A b_5 stimulated $k_{cat}/K_{m, CuOOH}$ by 3-fold. Interestingly, b_5 stimulated CuOOH-supported $k_{cat}/K_{m, CuOOH}$ by both increasing the k_{cat} and decreasing the $K_{m, CuOOH}$ values (Table 3 vs. Table 4).

T309A and T309V exhibit enhanced P450 3A4 activity with 7-BFC. The CYP3A4 random mutants were tested with 7-BFC in order to investigate whether the enhanced CuOOH-dependent activity with 7-BQ also was retained with a structurally distinct substrate. While T309A and T309V showed significantly increased activity with 7-BFC (at 75 μM) by 1.5- and 3.5-fold, respectively, the random mutants showed lower activity than CYP3A4 (data not shown). Therefore, steady-state kinetic analysis of 7-BFC *O*-deethylation with CYP3A4, T309A, and T309V was performed. The results are presented in Table 5. Interestingly, the $K_{m, CuOOH}$ for 7-BFC *O*-deethylation was 5-fold

lower than for 7-BQ debenzylation. T309V showed ~2.5-fold higher $k_{cat}/K_{m, CuOOH}$ for 7-BFC oxidation than CYP3A4. Furthermore, b_5 stimulated $k_{cat}/K_{m, CuOOH}$ for the oxidation of 7-BFC by > 7-fold for CYP3A4, whereas it stimulated $k_{cat}/K_{m, CuOOH}$ by 5- and 3-fold for T309A and T309V, respectively (Table 5). The b_5-mediated enhancement of $k_{cat}/K_{m, CuOOH}$ with 7-BFC was accomplished as the result of increased k_{cat} and decreased $K_{m, CuOOH}$. As seen earlier with 7-BQ, T309A and T309V also showed decreased k_{cat} in the NADPH-supported reaction with 7-BFC compared with CYP3A4 (data not shown).

T433S exhibits enhanced activity with testosterone. The CYP3A4 random mutants were also assayed with another structurally distinct substrate, testosterone. CYP3A4 yielded 6β-hydroxytestosterone as the major (92%) and 2β-hydroxytestosterone as a minor metabolite. The metabolite profile was unchanged in random mutants and T309A, whereas T309V yielded ~30% 2β-hydroxy testosterone. Although most of the mutants showed decreased testosterone 6β-hydroxylation, T433S showed a > 1.5-fold higher activity at 200 μM substrate than CYP3A4. Therefore, steady-state kinetic analysis of testosterone 6β-hydroxylation by CYP3A4 and T433S was performed, and the results are presented in Table 6. Interestingly, the $K_{m, CuOOH}$ for testosterone hydroxylation was > 3-fold lower than for 7-BQ debenzylation. T433S showed a > 3-fold higher $k_{cat}/K_{m, CuOOH}$ than CYP3A4 for testosterone 6β-hydroxylation as the result of increased k_{cat} and decreased $K_{m, CuOOH}$. Cytochrome b_5 further stimulated $k_{cat}/K_{m, CuOOH}$ by > 5-fold by increasing the k_{cat} and decreasing the $K_{m, CuOOH}$ values. In the NADPH system T433S showed a > 2-fold higher k_{cat} than CYP3A4 with unaltered $S_{50, 7\text{-BQ}}$ and n values (Table 6). Other mutants, however, showed either similar or lower k_{cat} than CYP3A4 (data not

shown). The results suggested that Thr^{433}→Ser substitution is unique in that it enhances CuOOH- and NADPH-supported reactions with testosterone, but not with 7-BQ or 7-BFC.

Synthesis of 6β-OH testosterone by T433S in the presence of cytochrome *b*$_5$. The decrease in the $K_{m,\ CuOOH}$ with testosterone T433S and upon b_5 addition is very important, because CuOOH also depletes the heme in a time- and concentration-dependent manner. Therefore, it was critical to find the optimal CuOOH concentrations at which T433S can convert testosterone into 6β-OH testosterone. CuOOH concentration-dependent heme depletion was examined at different time intervals (1-60 min), and the rate constants for P450 inactivation were determined (Fig. 3). Subsequently, a re-plot of k_{inact} and CuOOH concentrations using the Michaelis-Menten equation was carried out, which gave a $K_{I,\ CuOOH}$ of 6.5 mM (Fig. 3). The $K_{I,\ CuOOH}$ for heme depletion is > 10-fold higher than the $K_{m,\ CuOOH}$ for testosterone hydroxylation. Therefore, lower concentrations (0.1 to 0.25 mM) of CuOOH should be suitable for longer incubations to achieve nearly complete product formation.

A time course experiment with CYP3A4 and T433S in the absence and presence of b_5 containing 50 μM testosterone, 0.25 μM of CYP3A4 and b_5, and 0.2 mM CuOOH was carried out (Fig. 4). The results showed that T433S in the presence of b_5 converts ~75% of testosterone to 6β-OH testosterone in 2 h. On the other hand, CYP3A4 in the absence of b_5 converts only ~5% to 6β-OH testosterone in 2 h. Furthermore, to test whether the percent formation of 6β-OH testosterone was reduced when the reaction volume was increased, 0.1, 1.0, and 10-ml reactions were carried out in a container with a

large surface area, and with occasional mixing. The results showed that there was only a modest decrease in the percent conversion when the reaction volume was increased by 100-fold (data not shown).

Discussion

As a complement to the standard reconstituted system, which requires CPR, b_5, and the expensive cofactor, NADPH, we engineered CYP3A4 using random and site-directed mutagenesis for peroxide-supported activity. The engineered enzymes can utilize CuOOH more efficiently than CYP3A4 wild-type to metabolize several substrates such as 7-BQ, 7-BFC, and testosterone. Random mutagenesis yielded mutants (L216W, F228I, F241V, and T433S) outside of the active site, whereas by site-directed mutagenesis active site mutants T309A and T309V were produced (Figure 5). This is the first report on the engineering of CYP3A4 for enhanced utilization of an alternate oxygen donor. Although combination of single random mutants did not enhance $k_{cat}/K_{m,\ CuOOH}$ further, combination of a random and a site-directed mutant yielded F228I/T309A, which displays an 11-fold higher $k_{cat}/K_{m,\ CuOOH}$ than CYP3A4 for 7-BQ debenzylation. While directed evolution yielded mutants without a significant effect on P450 expression or stability, site-directed mutants showed decreased P450 expression and stability. Therefore, one advantage of directed evolution from the standpoint of generating novel catalysts for industrial applications is that only mutants with good expression levels and stability are isolated in the whole-cell screens (Kumar et al., 2005a; Kumar and Halpert, 2005). In contrast, site-directed mutagenesis often yields mutants with decreased expression and/or stability, especially when multiple substitutions are combined (Kumar et al., 2003; Kumar and Halpert, 2005). Thus directed evolution allows us to screen for mutants with enhanced activity that retain expression and stability.

The general mechanism by which peroxide supports P450-mediated substrate oxidation remains unclear, because significant activity requires an appropriate

cytochrome P450, substrate, and peroxide. An X-ray crystal structure of CYP3A4 suggests that Arg-212 may provide general base catalysis of peroxide cleavage (Yano et al., 2004). Therefore, replacement by a non-basic residue may decrease or even eliminate such activity. To explore this hypothesis we probed H_2O_2-supported oxidation of 7-BQ by R212A. However, there was no significant effect of this replacement on k_{cat} (data not shown). Based on the crystal structure of P450eryF T252A, the conserved threonine is thought to be involved in proton delivery to the oxygen species (Raag et al., 1991). It has been hypothesized that P450 can deploy three different oxygenating species (peroxo, hydroperoxo, and oxenoid-iron), and they prefer certain types of reactions (Keizers et al., 2005). Furthermore, based on enhanced CuOOH-supported and decreased NADPH-supported activity by T309A in CYP2D6 it was suggested that the mutant predominantly forms the peroxo and/or hydroperoxo complexes as opposed to oxenoid-iron complex, which is mainly preferred by the NADPH-dependent reaction in the wild-type. Similarly, the finding that T309V and T309A in CYP3A4 exhibited increased CuOOH- and decreased NADPH-supported activity compared with CYP3A4 is consistent with the hypothesis that the mutants predominantly form peroxo and/or hydroperoxo complexes. In contrast, the corresponding T302A in CYP2B4 and T303A in CYP2E1 showed decreased peroxide-dependent activity with one substrate but increased activity with another substrate (Vaz et al., 1996; Vaz et al., 1998), which is consistent with our observations that CYP3A4 T309V showed decreased CuOOH-supported activity with testosterone, but not with 7-BQ or 7-BFC.

Another important observation in this study suggests that the $K_{m,\ CuOOH}$ is dependent on the substrate used. In the absence of b_5 the $K_{m,\ CuOOH}$ is 1.2 mM, 0.22 mM,

and 0.38 mM for the oxidation of 7-BQ, 7-BFC, and testosterone, respectively. The $K_{m, CuOOH}$ for P450 is usually associated with the accessibility of CuOOH to the active site heme pocket (Zhang and Pernecky, 1999). Removal of the NH_2-terminal region in P450 2B4 caused a 5-fold decrease in $K_{m, CuOOH}$ for N-methylaniline demethylation, suggesting that the N-terminal region might mask the accessibility of CuOOH in the active site (Zhang and Pernecky, 1999). However, the mechanism by which substrates alter CuOOH accessibility is rather unclear. More recently, our laboratory has proposed that binding of a second molecule of substrate that shows homotropic cooperativity, such as 1-pyrenebutanol, induces a conformational transition in CYP3A4 that appears to close the heme pocket (Davydov et al., 2005) (unpublished observations). This phenomenon does not appear to occur when only one molecule of bromocriptine binds to CYP3A4. Therefore, we speculate that 7-BQ, which shows a higher extent of cooperativity than 7-BFC or testosterone (Harlow and Halpert, 1998; Domanski et al., 2001) (Table 1), masks the active site for the access of CuOOH leading to an increased $K_{m,CuOOH}$.

Our results from the peroxide-supported reaction suggest that L216W and F228I play a major role in enhancing catalytic efficiency of 7-BQ debenzylation. X-ray crystal structures (Figure 5) and extensive site-directed mutagenesis do not predict a role of these non-active site residues in substrate binding and/or metabolism (Domanski and Halpert, 2001; Hutzler and Tracy, 2002; Ekins et al., 2003; Tanaka et al., 2004; Williams et al., 2004; Yano et al., 2004; Park et al., 2005; Scott and Halpert, 2005). However, recent molecular dynamics simulations with the newly developed force field parameters for the heme-thiolate group and its dioxygen adduct show differences in structural and dynamic properties between CYP3A4 in the resting form and its complexes with the substrate

progesterone and the inhibitor metyrapone (Park et al., 2005). The results indicated that the broad substrate specificity of CYP3A4 stems from the malleability of a loop (residues 211-218) that resides in the vicinity of the channel connecting the active site and bulk solvent. Interestingly, L216W (F-helix) and F228I (F-G loop) mutations are located in or close to this region, which may cause a conformational transition upon 7-BQ binding leading to enhanced peroxide-supported reactions. Phe-241 is located in the G-helix, and its role in substrate binding or metabolism is not clear. Thr-433 is located near the most conserved region Cys-442, which ligates the heme iron as the 5th ligand.

Although, the role of b_5 as a source of electrons for P450 is well known (Schenkman and Jansson, 2003), increasing evidence points to a modulatory effect of b_5 mediated by a conformational transition in P450 (Reed and Hollenberg, 2003; Yamaori et al., 2003; Yamaguchi et al., 2004). Recently, we have shown that b_5 stimulates H_2O_2-supported 7-BQ debenzylation by CYP3A4 (Kumar et al., 2005b). In addition, an independent finding has shown that b_5 directly induces positive cooperativity and enhances catalytic turnover of CYP3A4 with multiple substrates (Jushchyshyn et al., 2005). In the present study, a ~3-fold increase in the k_{cat} and ~2-fold decrease in the $K_{m, CuOOH}$ for the oxidation of 7-BQ, 7-BFC, and testosterone further suggests that b_5 plays a major role in modulating CYP3A4 activity. Earlier, it has been proposed that b_5 induces some reorganization in the heme moiety and substrate binding pocket of P450 2B4 that favors the binding of peroxide and benzphetamine (Aplentalina and Davydov, 1997). Therefore, we suggest that b_5 reorganizes the CYP3A4 active site heme pocket, which leads to a decreased $K_{m, CuOOH}$ by favoring the binding of CuOOH. Because the random mutants reside outside of the active and b_5 binding sites (Bridges et al., 1998; Schenkman

and Jansson, 2003; Williams et al., 2004; Yano et al., 2004), these mutations do not primarily alter the b_5-P450 interaction. In contrast, a reduced b_5-stimulated P450 activity in T309V is similar to earlier observations that I301F and A305F, which are closest to the heme (Williams et al., 2004; Yano et al., 2004), show impaired b_5-interaction (Kumar et al., 2005b). To further test the hypothesis that the b_5-P450 interaction is impaired in T309V, but not in random mutants, the K_d values for b_5 were determined in CYP3A4, T309V, and F228I at 0.25 μM protein concentration as described previously (Kumar et al., 2005b). The K_d for b_5 in T309V (0.30 μM) was increased by 6-fold compared with CYP3A4 (0.05 μM), whereas the K_d for b_5 in F228I (0.04 μM) was similar to that of CYP3A4 (data not shown).

An interest in producing large quantities of P450-mediated drug metabolites prompted us to find a simple and cost-effective way to synthesize such compounds. In a recent study, microsomal CYP3A4 from human liver or recombinant sources and a NADPH regenerating system have been used to produce ~50 mg of 6β-OH testosterone with 70% conversion to product (Vail et al., 2005). Consistent with the above studies, our data predict that in a one liter reaction with CuOOH, T433S in the presence of b_5 can produce ~10 mg of 6β-OH testosterone with 60% conversion to product. Although the yield using CuOOH is lower than the standard method, it is more cost effective. More recently, CYP2D6 and CYP3A4 have been identified and further optimized to utilize a selected peroxide donor such as CuOOH with improved activity compared with the standard NADPH reconstitution system (Chefson et al., 2006).

In summary, the directed evolution approach created CYP3A4 mutants with enhanced utilization of peroxide, while site-directed mutants T309A and T309V

specifically showed enhanced CuOOH-supported activity with 7-BQ and 7-BFC. Combination of the site-directed and random mutants created the most efficient enzyme, F228I/T309A, for peroxide-mediated oxidation of several substrates. Addition of b_5 further stimulated the k_{cat}/K_m for CuOOH-supported CYP3A4 activity, and the CYP3A4 random mutant T433S showed enhanced CuOOH- and NADPH-supported activity with testosterone. The mutations found in this study may be useful for re-engineering other related mammalian P450s for enhanced utilization of peroxide. In addition, this approach may be used to engineer xenobiotic-metabolizing P450 enzymes for facile synthesis of milligram quantities of specific drug metabolites, agrochemicals, and food ingredients, and for bioremediation.

Acknowledgements

The authors thank Drs. Frances H. Arnold and Edgardo Farinas from California Institute of Technology, CA for providing technical details of directed evolution and sharing their unpublished materials. We thank Dr. Dmitri Davydov for his expert suggestions, Dr. B. K. Muralidhara for generating Figure 5, and Ms. You-Qun He for technical support in optimizing error-prone PCR. We also thank Dr. Richard Hodge, Synthetic Organic Chemistry Core Laboratory, UTMB, for synthesizing 7-BQ, and Dr. Kenneth Johnson, Pharmacology and Toxicology, UTMB, for allowing us to use their fluorescence plate reader (Ascent).

References

Aplentalina EV and Davydov DR (1997) Effect of cytochrome b(5) on thermodynamic parameters pf substrate binding and spin transitions in cytochrome P450 2B4. *FASEB J* **11**:A791-A791 P116.

Bridges A, Gruenke L, Chang YT, Vakser IA, Loew G and Waskel L (1998) Identfication of the binding site on cytochrome P450 2B4 for cytochrome b5 and cytochrome P450 reductase. *J Biol Chem* **273:**17036-17049.

Chefson A, Zhao J and Auclair K (2006) Replacement of natural cofactors by selected hydrogen peroxide donors or organic peroxides results in improved activity for CYP3A4 and CYP2D6. *Chembiochem* **7:**916-919.

Cirino PC, Mayer KM and Umeno D (2003) Generating mutant libraries using error-prone PCR. *Methods Mol Biol* **231:**3-9.

Coon MJ (2005) Cytochrome P450: nature's most versatile biological catalyst. *Ann Rev Pharmacol Toxicol* **45:**1-25.

Davydov DR, Fernando H, Baas BJ, Sligar SG and Halpert JR (2005) Kinetics of dithionite-dependent reduction of cytochrome P450 3A4: heterogeneity of the enzyme caused by its oligomerization. *Biochemistry* **44:**13902-13913.

DeLano, WL (2004) *The PyMol User's Manual*, DeLano Scientific LLC, San Carlos, CA.

Domanski TL and Halpert JR (2001) Analysis of mammalian cytochrome P450 structure and function by site-directed mutagenesis. *Curr Drug Metab* **2:**117-137.

Domanski TL, He YA, Khan KK, Roussel F, Wang Q and Halpert JR (2001) Phenylalanine and tryptophan scanning mutagenesis of CYP3A4 substrate

recognition site residues and effect on substrate oxidation and cooperativity. *Biochemistry* **40:**10150-10160.

Ekins S, Stresser DM and J. AW (2003) In vitro and pharmacophore insights into CYP3A enzymes. *Trends Pharmacol Sci* **24:**161-166.

Gillam EM (2005) Exploring the potential of xenobiotic-metabolising enzymes as biocatalysts: evolving designer catalysts from polyfunctional cytochrome P450 enzymes. *Clin Exp Pharmacol Physiol* **32:**147-152.

Glieder A, Farinas ET and Arnold FH (2002) Laboratory evolution of a soluble, self-sufficient, highly active alkane hydroxylase. *Nat Biotechnol* **20:**1135-1139.

Guengerich FP (1999) Cytochrome P-450 3A4: regulation and role in drug metabolism. *Ann Rev Pharmacol Toxicol* **39:**1-17.

Harlow GR and Halpert JR (1997) Alanine-scanning mutagenesis of a putative substrate recognition site in human cytochrome P450 3A4. Role of residues 210 and 211 in flavonoid activation and substrate specificity. *J Biol Chem* **272:**5396-5402.

Harlow GR and Halpert JR (1998) Analysis of human cytochrome P450 3A4 cooperativity: construction and characterization of a site-directed mutant that displays hyperbolic steroid hydroxylation kinetics. *Proc Natl Acad Sci USA* **95:**6636-6641.

Hutzler JM and Tracy TS (2002) Atypical kinetic profiles in drug metabolism reactions. *Drug Metab Dispos* **30:**355-362.

Jushchyshyn MI, Hutzler JM, Schrag ML and Wienkers LC (2005) Catalytic turnover of pyrene by CYP3A4: evidence that cytochrome b5 directly induces positive cooperativity. *Arch Biochem Biophys* **438:**21-28.

Keizers PH, Schraven LH, de Graaf C, Hidestrand M, Ingelman-Sundberg M, van Dijk BR, Vermeulen NP and Commandeur JN (2005) Role of the conserved threonine 309 in mechanism of oxidation by cytochrome P450 2D6. *Biochem Biophys Res Commun* **338:**1065-1074.

Kim D and Guengerich FP (2004) Enhancement of 7-methoxyresorufin O-demethylation activity of human cytochrome P450 1A2 by molecular breeding. *Arch Biochem Biophys* **432:**102-108.

Kumar S, Chen CS, Waxman DJ and Halpert JR (2005a) Directed evolution of mammalian cytochrome P450 2B1: mutations outside of the active site enhance the metabolism of several substrates, including the anticancer prodrugs cyclophosphamide and ifosfamide. *J Biol Chem* **280:**19569-19575.

Kumar S, Davydov DR and Halpert JR (2005b) Role of cytochrome B5 in modulating peroxide-supported CYP3A4 activity: evidence for a conformational transition and cytochrome P450 heterogeneity. *Drug Metab Dispos* **33:**1131-1136.

Kumar S and Halpert JR (2005) Use of directed evolution of mammalian cytochromes P450 for investigating the molecular basis of enzyme function and generating novel biocatalysts. *Biochem Biophys Res Commun* **338:**456-464.

Kumar S, Scott EE, Liu H and Halpert JR (2003) A rational approach to re-engineer cytochrome P450 2B1 regioselectivity based on the crystal structure of P450 2C5. *J Biol Chem* **278:**17178-17184.

Meinhold P, Peters MW, Chen MM, Takahashi K and Arnold FH (2005) Direct conversion of ethane to ethanol by engineered cytochrome P450 BM3. *Chembiochem* **6:**1765-1768.

Nebert DW and Russell DW (2002) Clinical importance of the cytochromes P450. *Lancet* **360:**1155-1162.

Otey CR, Bandara G, Lalonde J, Takahashi K and Arnold FH (2006) Preparation of human metabolites of propranolol using laboratory-evolved bacterial cytochromes P450. *Biotechnol Bioeng* **93:**494-499.

Park H, Lee S and Suh J (2005) Structural and dynamical basis of broad substrate specificity, catalytic mechanism, and inhibition of cytochrome P450 3A4. *J Am Chem Soc* **127:**13634-13642.

Raag R, Martinis SA, Sligar SG and Poulos TL (1991) Crystal structure of the cytochrome P-450CAM active site mutant Thr252Ala. *Biochemistry* **30:**11420-11429.

Reed JR and Hollenberg PF (2003) Comparison of substrate metabolism by cytochromes P450 2B1, 2B4, and 2B6: relationship of heme spin state, catalysis, and the effects of cytochrome b5. *J Inorg Biochem* **93:**152-160.

Schenkman JB and Jansson I (2003) The many roles of cytochrome b5. *Pharmacol Ther* **97:**139-152.

Schoemaker HE, Mink D and Wubbolts MG (2003) Dispelling the myths--biocatalysis in industrial synthesis. *Science* **299:**1694-1697.

Scott EE and Halpert JR (2005) Structures of cytochrome P450 3A4. *Trends Biochem Sci* **30:**5-7.

Tanaka T, Okuda T and Yamamoto Y (2004) Characterization of the CYP3A4 active site by homology modeling. *Chem Pharm Bull (Tokyo)* **52:**830-835.

Vail RB, Homann MJ, Hanna I and Zaks A (2005) Preparative synthesis of drug metabolites using human cytochrome P450s 3A4, 2C9 and 1A2 with NADPH-P450 reductase expressed in Escherichia coli. *J Ind Microbiol Biotechnol* **32:**67-74.

Vaz AD, McGinnity DF and Coon MJ (1998) Epoxidation of olefins by cytochrome P450: evidence from site-specific mutagenesis for hydroperoxo-iron as an electrophilic oxidant. *Proc Natl Acad Sci USA* **95:**3555-3560.

Vaz AD, Pernecky SJ, Raner GM and Coon MJ (1996) Peroxo-iron and oxenoid-iron species as alternative oxyegenating agents in cytochrome P450-catalyzed reactions: switching by threonin-302 to alanine mutagenesis of cytochrome P450 2B4. *Proc Natl Acad Sci USA* **93:**4644-4648.

Williams PA, Cosme J, Vinkovic DM, Ward A, Angove HC, Day PJ, Vonrhein C, Tickle IJ and Jhoti H (2004) Crystal structures of human cytochrome P450 3A4 bound to metyrapone and progesterone. *Science* **305:**683-686.

Yamaguchi Y, Khan KK, He YA, He YQ and Halpert JR (2004) Topological changes in the CYP3A4 active site probed with phenyldiazene: effect of interaction with NADPH-cytochrome P450 reductase and cytochrome b5 and of site-directed mutagenesis. *Drug Metab Dispos* **32:**155-161.

Yamaori S, Yamazaki H, Suzuki A, Yamada A, Tani H, Kamidate T, Fujita K and Kamataki T (2003) Effects of cytochrome b(5) on drug oxidation activities of human cytochrome P450 (CYP) 3As: similarity of CYP3A5 with CYP3A4 but not CYP3A7. *Biochem Pharmacol* **66:**2333-2340.

Yano JK, Wester MR, Schoch GA, Griffin KJ, Stout CD and Johnson EF (2004) The structure of human microsomal cytochrome P450 3A4 determined by X-ray crystallography to 2.05-A resolution. *J Biol Chem* **279:**38091-38094.

Zhang Y and Pernecky SJ (1999) Cumene hydroperoxide-supported demethylation reactions catalyzed by cytochrome P450 2B4 lacking the NH2-terminal sequence. *Biochem Biophys Res Commun* **258:**32-38.

Footnotes

a) This work was supported by National Institutes of Health grants GM54995 and Center Grant ES06676. This work was partially presented at Experimental Biology 2006, San Francisco, CA, and the 5th SW P450 meeting, 2006, Navasota, TX.

b) Reprint requests should be sent to: Dr. Santosh Kumar, Department of Pharmacology and Toxicology, University of Texas Medical Branch, 301 University Boulevard, Galveston, TX 77555-1031. Tel: (409) 772-9677, Fax: (409) 772-9642, Email: sakumar@utmb.edu

Legends for figures

Figure 1. Primers for the construction of CYP3A4 random and site-directed mutants. The codons that were changed to make the desired mutation are shown in bold. [1]These mutants were created by random mutagenesis using error-prone PCR of the cDNA of CYP3A4, as described in Materials and Methods.

Figure 2. Development of screening and selection. A. Diamonds and Triangles represent the activities with 7-BQ determined for individual clones from negative control (plasmid only) and CYP3A4 wild-type, respectively, and are plotted in random distribution of the activity to demonstrate the range across the 96-well microplate. B. The activities of individual clones of randomly mutagenized CYP3A4 are plotted in decreasing order of activity. The X-axis represents individual colonies, and the Y-axis represents relative fluorescence intensity for the product, 7-HQ, at λ_{ex} = 405 nm and λ_{em} = 510 nm.

Figure 3. P450 3A4-heme depletion assays at different concentrations of CuOOH and 0.25 μM P450 as described in Materials and Methods. The plot represents the percent P450 (Y axis) as a function of incubation time (X axis) at increasing concentrations of CuOOH. The plots of the fit to a first-order equation yielded kinetic parameters as follows: 0.00 mM (k_{inact} = 0.003 min^{-1}), 0.05 mM (k_{inact} = 0.004 min^{-1}), 0.10 mM (k_{inact} = 0.016 min^{-1}), 0.25 mM (k_{inact} = 0.020 min^{-1}), 0.50 mM (k_{inact} = 0.046 min^{-1}), 2.0 mM (k_{inact} = 0.070 min^{-1}), 5.0 mM (k_{inact} = 0.110 min^{-1}), 10 mM (k_{inact} = 0.180 min^{-1}), and 15 mM (k_{inact} = 0. 203 min^{-1}). The plot is representative of two independent experiments.

Figure 4. CuOOH-dependent formation of 6β-OH testosterone by CYP3A4 and T433S in the absence and presence of cytochrome b_5. Reactions were carried out at different time intervals, and product formation was measured as described in Materials and Methods. Error bars represent the mean ± S.D (n = 3).

Figure 5. Ribbon schematic representation of a three-dimentional structure of CYP3A4. The heme porphyrin (red sticks), heme iron (red sphere), and mutant residues (orange spheres) are shown. The structure was generated using the PDB ID 1TQN (Yano et al., 2004) and PyMol graphics (DeLano, 2004).

Table 1. Steady-state kinetics: H_2O_2- and NADPH-supported oxidation of 7-BQ by CYP3A4 and random mutants

H_2O_2-supported			
CYP3A4	k_{cat} (min^{-1})	$S_{50,\ 7\text{-BQ}}$ (μM)	n
WT	1.6 ± 0.06	105 ± 7.0	2.1 ± 0.10
L216W	2.6 ± 0.17	139 ± 5.2	1.8 ± 0.06
F241V	1.9 ± 0.04	107 ± 3.4	2.3 ± 0.14
F228I	2.9 ± 0.60	161 ± 52	1.2 ± 0.13
T433S	2.7 ± 0.80	95.2 ± 14	1.7± 0.12
NADPH-supported			
CYP3A4	k_{cat} (min^{-1})	$S_{50,\ 7\text{-BQ}}$ (μM)	n
WT	43 ± 14	228 ± 60	2.8 ± 0.32
L216W	37 ± 10	276 ± 60	2.2 ± 0.31
F241V	25 ± 6.0	158 ± 30	3.1 ± 0.33
F228I	29 ± 8.9	316 ± 14	1.0 ± 0.10
T433S	39 ± 10	132 ± 11	1.5 ± 0.14

Results are the mean ± standard deviation of at least three independent experiments.

DMD Fast Forward. Published on September 20, 2006 as DOI: 10.1124/dmd.106.012054
This article has not been copyedited and formatted. The final version may differ from this version.

Table 2. Steady-state kinetics: H_2O_2-supported oxidation of 7-BQ by CYP3A4 and site-directed and random mutants

CYP3A4	k_{cat} (min^{-1})	$K_{m,\ HOOH}$ (mM)	k_{cat}/K_m
WT	7.6 (1.5) [a]	61 (15)	0.12
L216W	7.6 (2.0)	22 (10)	0.34
F241V	7.0 (2.4)	44 (21)	0.16
F228I	6.7 (0.71)	21 (3.8)	0.32
T433S	4.9 (1.0)	26 (9.0)	0.19
L216W/F241V	2.5 (0.24)	18 (4.3)	0.14
F228I/T433S	8.6 (2.2)	32 (12)	0.27
L216W/F228I	3.9 (0.76)	28 (4.3)	0.14
F241V/F228I	7.9 (1.0)	26 (11)	0.30
F241V/T433S	3.2 (0.15)	23 (2.4)	0.14
L216W/F228I/T433S	9.0 (2.4)	41 (22)	0.22

Results are representative of at least two independent determinations. The variation between the experiments is ≤ 20%. For steady-state kinetic analysis 1 - 25 mM of H_2O_2 was used.

[a] Standard errors for fit to Michaelis-Menten are shown in parenthesis.

DMD Fast Forward. Published on September 20, 2006 as DOI: 10.1124/dmd.106.012054
This article has not been copyedited and formatted. The final version may differ from this version.

Table 3. Steady-state kinetics: CuOOH-supported oxidation of 7-BQ by CYP3A4 and site-directed and random mutants

CYP3A4	k_{cat} (min^{-1})	$K_{m,\ CuOOH}$ (mM)	k_{cat}/K_m
WT	1.2 (0.06) [a]	1.2 (0.10)	1.0
T309A	6.0 (1.0)	1.2 (0.14)	5.0
T309V	8.9 (1.5)	1.4 (0.12)	6.4
L216W	1.4 (0.12)	0.44 (0.12)	3.2
F241V	2.2 (0.09)	1.0 (0.12)	2.2
F228I	3.0 (0.16)	0.70 (0.11)	4.3
T433S	2.5 (0.09)	1.3 (0.13)	1.9
L216W/F241V	1.8 (0.10)	1.4 (0.2)	1.3
F228I/T433S	1.3 (.09)	1.0 (0.19)	1.3
L216W/F228I	2.7 (0.20)	1.8 (0.38)	1.5
F241V/F228I	4.5 (0.29)	2.6 (0.35)	1.7
F241V/T433S	3.2 (0.15)	2.3 (0.24)	1.4
L216W/F228I/T433S	2.5 (0.26)	1.2 (0.30)	2.1
L216W/T309A	5.6 (0.29)	0.70 (0.07)	8.0
F228I/T309A	7.8 (0. 50)	0.73 (0.15)	11

Results are representative of at least two independent determinations. The variation between the experiments is ≤ 15%.

[a] Standard errors for fit to Michaelis-Menten are shown in parenthesis.

Table 4. Steady-state kinetics: CuOOH-supported oxidation of 7-BQ by CYP3A4 and site-directed and random mutants in the presence of cytochrome b_5

CYP3A4	k_{cat} (min^{-1})	$K_{m,\ CuOOH}$ (mM)	k_{cat}/K_m
WT	3.9 (0.23)[a]	0.54 (0.05)	7.2
L216W	4.1 (0.29)	0.31 (0.04)	13
F228I	4.0 (0.16)	0.41 (0.04)	9.7
T433S	6.0 (0.31)	0.49 (0.06)	7.6
T309A	9.0 (0.46)	0.52 (0.05)	17
T309V	11 (0.45)	1.2 (0.17)	9.1
F228I/T309A	18.0 (0.56)	0.60 (0.05)	30

Results are representative of at least two independent determinations. The variation between the experiments is ≤ 20%.

[a] Standard errors for fit to Michaelis-Menten are shown in parenthesis.

DMD Fast Forward. Published on September 20, 2006 as DOI: 10.1124/dmd.106.012054
This article has not been copyedited and formatted. The final version may differ from this version.

Table 5. Steady-state kinetics: CuOOH-supported oxidation of 7-BFC by CYP3A4 and mutants in the absence and in the presence of cytochrome b_5

CYP3A4	- b_5			+ b_5		
	k_{cat} (min^{-1})	$K_{m, CuOOH}$ (mM)	k_{cat}/K_m	k_{cat} (min^{-1})	$K_{m, CuOOH}$ (mM)	k_{cat}/K_m
WT	0.38 (0.02)[a]	0.22 (0.03)	1.7	1.2 (0.06)	0.10 (0.2)	12
T309A	0.45 (0.01)	0.19 (0.01)	2.4	1.9 (0.03)	0.11 (0.05)	17
T309V	1.1 (0.08)	0.27 (0.06)	4.1	2.1 (0.06)	0.19 (0.02)	11

Results are representative of at least two independent determinations. The variation between the experiments is ≤ 20%.

[a] Standard errors for fit to Michaelis-Menten are shown in parenthesis.

DMD Fast Forward. Published on September 20, 2006 as DOI: 10.1124/dmd.106.012054
This article has not been copyedited and formatted. The final version may differ from this version.

Table 6. Steady-state kinetics: CuOOH- and NADPH-supported 6β-hydroxylation of testosterone by CYP3A4 and T433S in the absence and in the presence of cytochrome b_5

CYP3A4	- b_5			+b_5		
CuOOH	k_{cat} (min^{-1})	$K_{m,\ CuOOH}$ (mM)	k_{cat}/K_m	k_{cat} (min^{-1})	$K_{m,\ CuOOH}$ (mM)	k_{cat}/K_m
WT	0.81 (0.09)[a]	0.38 (0.08)	2.1	1.9 (0.04)	0.15 (0.05)	13
T433S	1.6 (0.12)	0.24 (0.07)	6.7	2.8 (0.09)	0.09 (0.01)	31
NADPH	k_{cat} (min^{-1})		S_{50} (μM)		*n*	
WT	22.1 (1.5)		61.4 (7.6)		1.56 (0.16)	
T433S	47.6 (3.3)		65.3 (8.2)		1.56 (0.16)	

Results are representative of at least two independent determinations. The variation between the experiments is ≤ 20%.

[a] Standard errors for fit to Michaelis-Menten are shown in parenthesis.

Mutation	Template	Oligonucleotides
[1]L216W, F228I,	3A4	5’-CAC AGG AAA CAG ACC ATG GCT CCC AGT ATC-3’
F241V, T433S		5’-CGG ATATCA ATG GTG GTG ATG CCG AGC TGA GAA -3’
T309V	3A4	5’-TTTGCTGGCTAT**GAA**GTCACGAGCAGTGTT-3’ 5’-AACACTGCTCGTGA**CTT**CATAGCCAGCAAA-3’
L216W/F241V	F241V	5’-CTTTTAAGATTTGATTTT**TGG**GATCCATTCTTTCTC-3’ 5’-GAGAAAGAATGGATC**CCA**AAAATCAAATCTTAAAAG-3’
F228I/T433S	F228I	5’-GATCCTTACATATAC**TCA**CCCTTTGGAAGTGGA-3’ 5’-TCCACTTCCAAAGGG**TGA**GTATATGTAAGGATC-3’
L216W/F228I	F228I	5’-CTTTTAAGATTTGATTTT**TGG**GATCCATTCTTTCTC-3’ 5’-GAGAAAGAATGGATC**CCA**AAAATCAAATCTTAAAAG-3’
F241V/F228I	F228I	5’-GTATTAAATATCTGT**GTC**GTTCCAAGAGAAGTTACA-3’ 5’-TGTAACTTCTCTTGGAAC**GAC**ACAGATATTTAATAC-3’
F241V/T433S T433S		5’-GTATTAAATATCTGT**GTC**GTTCCAAGAGAAGTTACA-3’ 5’-TGTAACTTCTCTTGGAAC**GAC**ACAGATATTTAATAC-3’
L216W/F228I/T433S	F228I/T433S	5’-CTTTTAAGATTTGATTTT**TGG**GATCCATTCTTTCTC-3’ 5’-GAGAAAGAATGGATC**CCA**AAAATCAAATCTTAAAAG-3’
T309V/L216W	L216W	5’-TTTGCTGGCTAT**GAA**GTCACGAGCAGTGTT-3’ 5’-AACACTGCTCGTGAC**TTC**ATAGCCAGCAAA-3’
T309V/F228I	F228I	5’-TTTGCTGGCTAT**GAA**GTCACGAGCAGTGTT-3’ 5’-AACACTGCTCGTGAC**TTC**ATAGCCAGCAAA-3’
T309A/L216W	L216W	5’-TTTGCTGGCTAT**GAA**GTCACGAGCAGTGTT-3’ 5’-AACACTGCTCGTGAC**TTC**ATAGCCAGCAAA-3’
T309A/F228I	F241V	5’-TTTGCTGGCTAT**GAA**GTCACGAGCAGTGTT-3’ 5’-AACACTGCTCGTGAC**TTC**ATAGCCAGCAAA-3’

Figure 1

A. Control

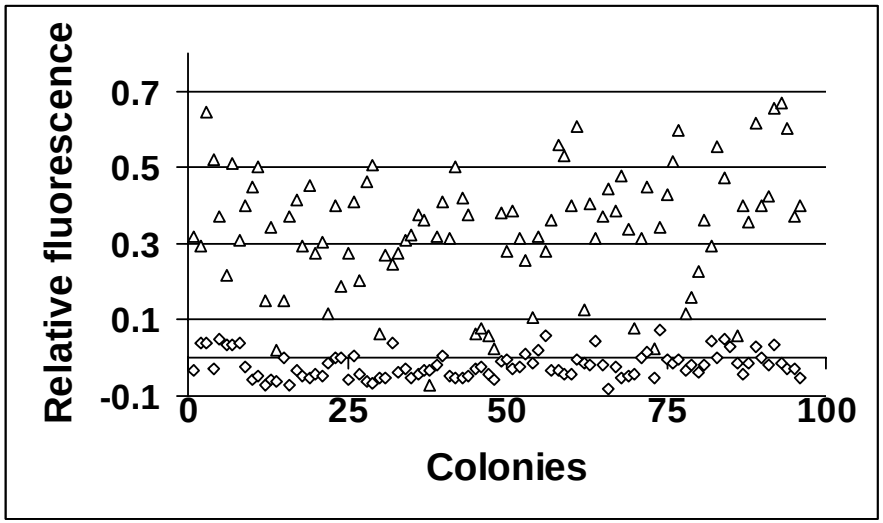

B. Random clones

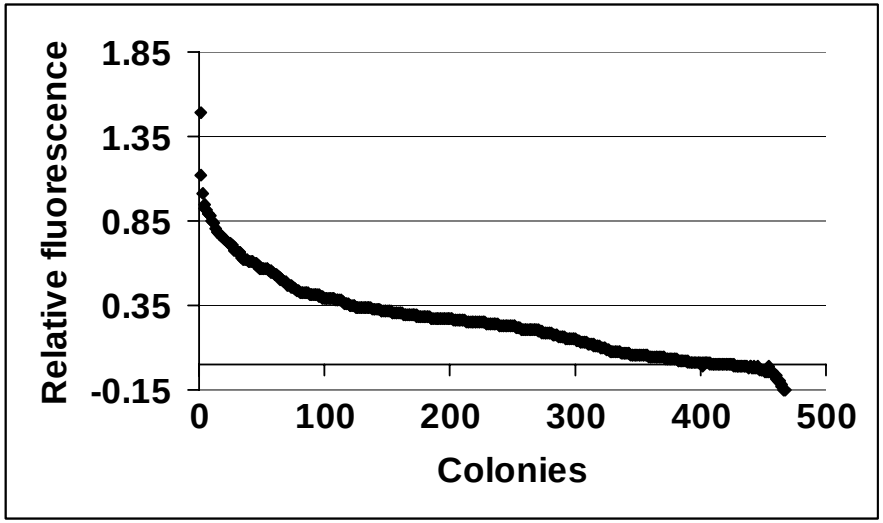

Figure 2

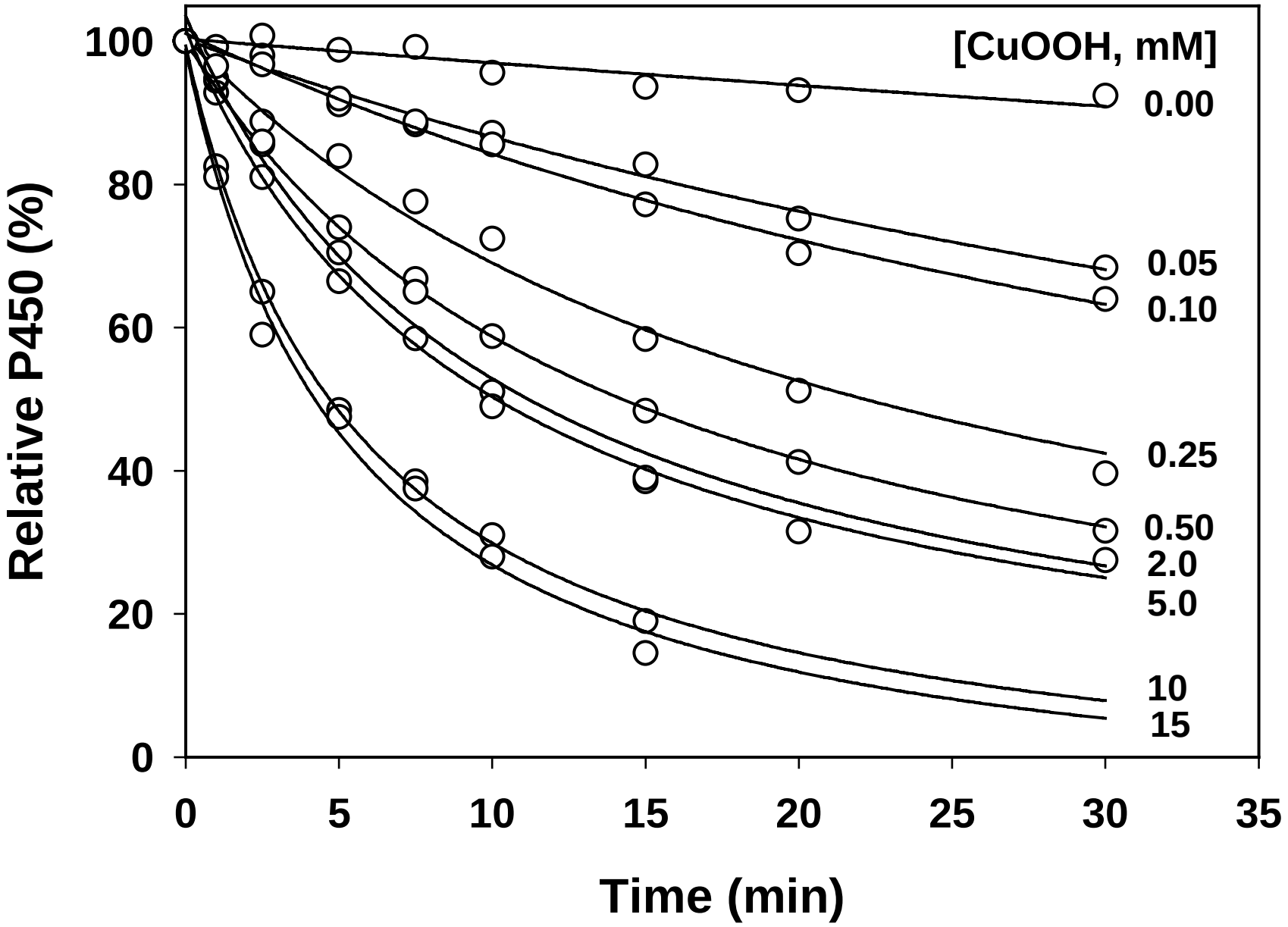

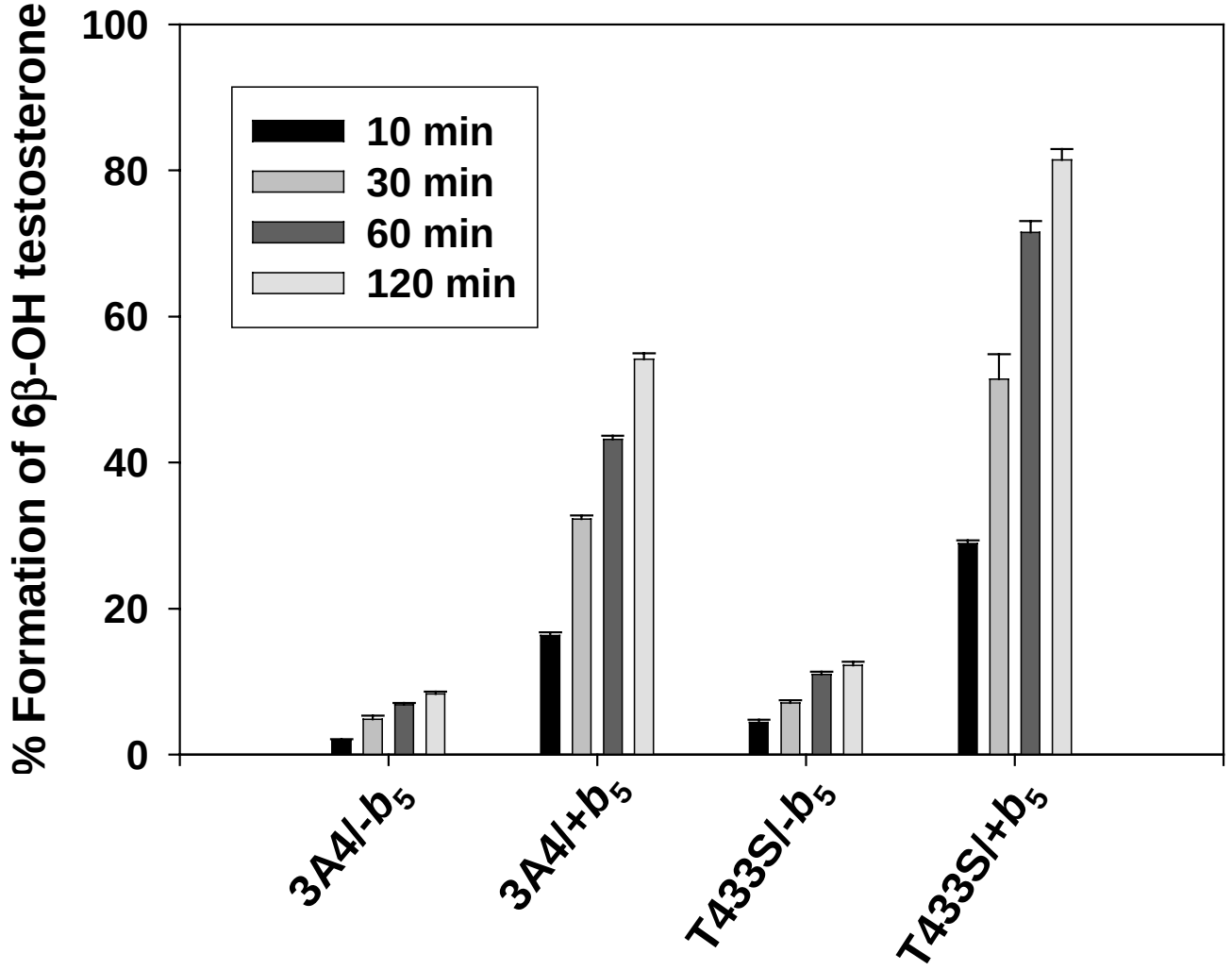

Figure 4

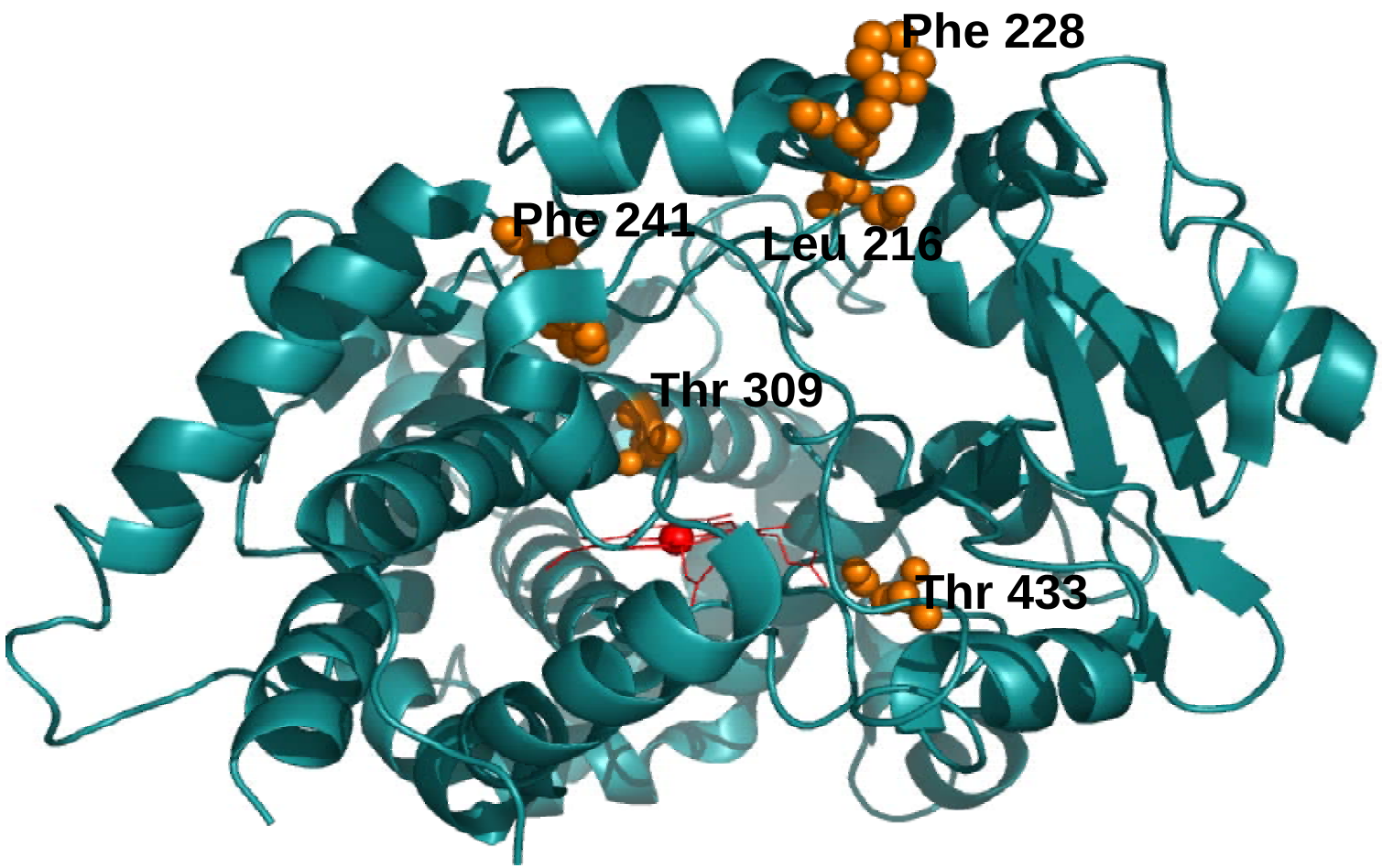

Figure 5